Nanocapsules

Deutsche Ausgabe: DOI: 10.1002/ange.201601140
Internationale Ausgabe: DOI: 10.1002/anie.201601140

Densely Packed Hydrophobic Clustering: Encapsulated Valerates Form a High-Temperature-Stable {Mo_{132}} Capsule System

*Somenath Garai, Hartmut Bögge, Alice Merca, Olga A. Petina, Alina Grego, Pierre Gouzerh, Erhard T. K. Haupt, Ira A. Weinstock, and Achim Müller**

Dedicated to Professor Herbert Roesky on the occasion of his 80th birthday

Abstract: *Porous molecular nanocontainers of {Mo_{132}}-type Keplerates offer unique opportunities to study a wide variety of relevant phenomena. An impressive example is provided by the highly reactive {Mo_{132}-CO_3} capsule, the reaction of which with valeric acid results in the very easy release of carbon dioxide and the uptake of 24 valerate ions/ligands that are integrated as a densely packed aggregate, thus indicating the unique possibility of hydrophobic clustering inside the cavity. Two-dimensional NMR techniques were used to demonstrate the presence of the 24 valerates and the stability of the capsule up to ca. 100°C. Increasing the number of hydrophobic parts enhances the stability of the whole system. This situation also occurs in biological systems, such as globular proteins or protein pockets.*

Despite the central role of the hydrophobic effect in a variety of biological processes,[1] hydrophobic clustering has not attracted significant research interest in non-biological fields. For a better understanding of the hydrophobic effect, deliberate studies can be performed under well-defined conditions inside the well-known porous metal-oxide-based capsules (also known as Keplerates) of the type $(pentagon)_{12}(linker)_{30} \equiv \{(M)M_5\}_{12}\{Mo_2(L,L)\}_{30}$ (M = Mo, W; (L,L) designates a bidentate or two monodentate ligands/functions; Figure 1).[2] {Mo_{132}}-type capsules are easily obtained simply by adding the dinuclear linker to a constitutional dynamic library of molybdates, which leads to "immediate" formation of the complementary pentagonal units.[3] The capsules show adaptive features and can easily be derivatized through building block and/or ligand/function exchange reactions, which allows tuning of the charge and softness, and especially fine tuning of the hydrophilicity/hydrophobicity of the inner walls.[2a,b] Mostly, these capsules have a reasonably large cavity connected to the outside through 20 crown ether type {Mo_9O_9} flexible pores[2a,b] that allow entry and exit of even comparably large guests[4] as well as stepwise closing and reopening.[5] Such features make them versatile platforms for detailed nanoscale studies of an exceptionally wide range of phenomena with chemical, physical, biological, or industrial relevance.[2a] Notably, they provide the opportunity to study hydrophobic interactions and clustering while removing hydrophobic toxic materials from water, as well as dewetting at the nanoscale.[6–8]

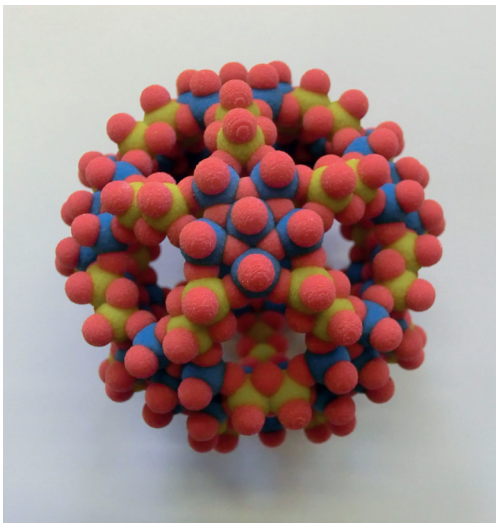

Figure 1. 3D artistic model (http://www.moleculart3d.com/) of the most celebrated {Mo_{132}} nanocapsule, a unique stable metal-oxide nanocluster (O red, Mo blue, functions yellow) that can provide the most versatile platform for studying the properties of matter under confined conditions.

We have recently focused on the influence of the length of the carbon chain on the integration of carboxylic acids within {Mo_{132}}-type capsules.[7,8] Carboxylic acids with different chain

[*] Dr. S. Garai, Dr. H. Bögge, Dr. A. Merca, Prof. Dr. A. Müller
Fakultät für Chemie, Universität Bielefeld
Postfach 100131, 33501 Bielefeld (Germany)
E-mail: a.mueller@uni-bielefeld.de
Dr. O. A. Petina
Forschungszentrum Jülich GmbH
INM-5, Wilhelm-Johnen-Straße, 52425 Jülich (Germany)
A. Grego, Prof. Dr. I. A. Weinstock
Department of Chemistry and
Ilse Katz Institute for Nanoscale Science and Technology
Ben-Gurion University of the Negev, Beer Sheva, 84105 (Israel)
Prof. Dr. P. Gouzerh
Institut Parisien de Chimie Moléculaire UMR CNRS 8232
Université Pierre et Marie Curie, Paris 06
4 place Jussieu, 75252 Paris (France)
Dr. E. T. K. Haupt
Universität Hamburg, Fachbereich Chemie
Institut für Anorganische und Angewandte Chemie
Martin-Luther-King-Platz 6, 20146 Hamburg (Germany)
Supporting information and ORCID(s) from the author(s) for this article are available on the WWW under: http://dx.doi.org/10.1002/anie.201601140.

lengths exert various biological functions, with the transmembrane transport of fatty acids being of special interest in context of the present work.[9–11] The design and synthesis of artificial receptors of long-chain fatty acids represents a difficult challenge.[12] A unique feature of $\{Mo_{132}\}$ capsules is their ability to integrate a large number of carboxylates, provided that the alkyl chains are not too long, while forming unprecedented assemblies (see Refs. [7] and [8] and below). It should be noted that the recovery of short-chain carboxylic acids, especially valeric acid, from aqueous wastes is of considerable importance from a health point of view.[13] Herein, we present the synthesis, X-ray crystal structure analysis, and detailed 2D NMR study of the valerate capsule in an effort to provide comparison with the encapsulation of smaller carboxylates, but also in the context of the removal of pollutants from water.

Compound **2** was prepared through the reaction of valeric acid with the carbonate-type precursor **1**. The latter has definite advantages over the acetate-type capsule that has most commonly been used in the past. Indeed, competition experiments demonstrate that replacement of the acetate ligands by increasingly larger carboxylate ions is hampered by increased steric hindrance. For example, this process is approximately five times less favorable for valerate than for butyrate (see Figure S1 in the Supporting Information). On the other hand, the carbonate-type $\{Mo_{132}\}$ capsule **1a**, which is moderately stable in aqueous solution only over a limited pH range, undergoes release of CO_2 upon acidification of the corresponding solution,[14] which leads to a highly reactive intermediate that is eager to entrap any ligand present. In the present case, encapsulation is further promoted by the tendency of valerate ions to aggregate through hydrophobic interactions with the capsule.

$(NH_4)_{72}[\{(Mo^{VI})Mo^{VI}_5O_{21}(H_2O)_6\}_{12}\ \{Mo^{V}_2O_4(CO_3)\}_{30}] \cdot$ ca. $280\,H_2O$ $\equiv (NH_4)_{72} \cdot$ **1a** $\cdot$ lattice ingredients $\equiv$ **1**[14]

$[(CH_3)_2NH_2]_{34}(NH_4)_2[\{(Mo^{VI})Mo^{VI}_5O_{21}(H_2O)_6\}_{12}\{Mo^{V}_2O_4(CH_3CH_2CH_2CH_2CO_2)\}_{24}\{Mo^{V}_2O_4(H_2O)_2\}_6] \cdot$ ca. $[3\,CH_3CH_2CH_2CH_2COO^- + 3\,NH_4^+ + 200\,H_2O] \equiv [(CH_3)_2NH_2]_{34}(NH_4)_2 \cdot$ **2a** $\cdot$ lattice ingredients $\equiv$ **2**

Compound **2** was characterized by elemental analysis, infrared (Figure S2 in the Supporting Information), Raman (Figure S3), and 1D and 2D ^{1}H NMR spectroscopy (Figure 3, Figure 4, Figure 5 and Figures S4–S8), and single-crystal X-ray diffraction.[15] The single-crystal X-ray structure analysis of **2** reveals the presence of the archetypal spherical cluster skeleton consisting of $12\,\{(Mo^{VI})Mo^{VI}_5O_{21}(H_2O)_6\}^{6-}$ pentagonal units positioned at the vertices of an icosahedron and connected by $30\,\{Mo^{V}_2O_2(\mu\text{-}O)_2\}^{2+}$ linkers (Figure 2a). Valerate ligands are coordinated to the linkers in the usual coordination mode, while forming a compact aggregate that occupies all internal space with the exception of a small empty (hydrophobic) cavity at the center of the capsule. The carbon chains are severely disordered, which makes it difficult to determine their exact number and orientations (Figure 2). Calculations using the program PLATON[16] support the presence of 24 valerate ligands within the capsule, which is in good agreement with the result obtained by NMR. Indeed, quantitative ^{1}H NMR spectroscopic analysis shows that **2** contains approximately 25 equivalents of valerate inside the capsule and 2 outside (with an uncertainty of ± 1). These values are rather close to those obtained for the butyrate capsule.[8a] The final refinement was done accordingly with 24 coordinated valerate ligands (C atoms of the carboxylate group have an 80% occupancy). A similar composition has been quite recently reported for a glutamate-type capsule.[17]

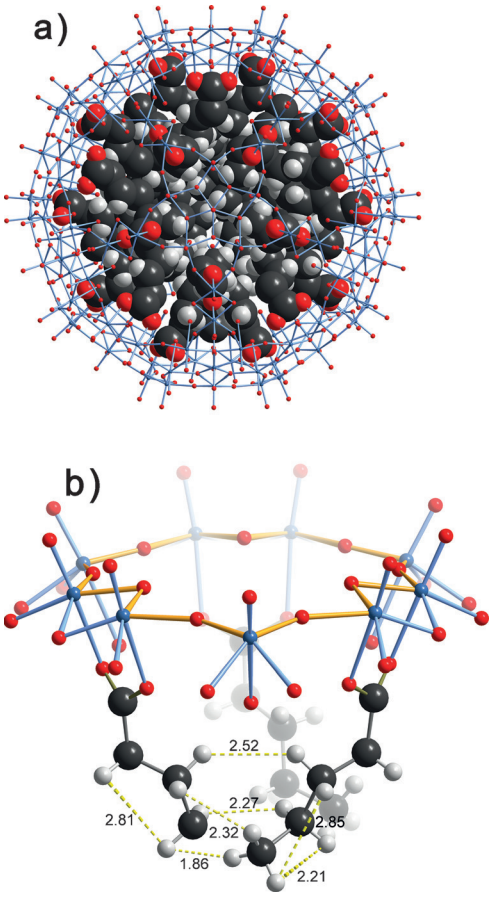

Figure 2. a) Structure of **2a** in a combined space-filling/ball-and-stick representation, with dense packing of the hydrophobic valerates (mainly disordered) inside the confined space of the nanosized metal-oxide skeleton. b) Side view of a $\{Mo_9O_9\}$ pore, emphasizing the short distances between the H atoms. The fifth C atom of the left valerate ligand could not be located crystallographically. Mo blue, O red, C black, H gray; yellow dashed lines indicate the above mentioned short distances.

Besides the signal due to dimethylammonium ions, the ^{1}H NMR spectrum of **2** dissolved in D_2O (Figure 3) shows four sharp signals that reveal the presence of some "free" valerates together with four significantly broadened signals. Peak broadening is generally observed as a consequence of restricted mobility for any of the species, such as carboxylates[4,7,8,18] and carbonate[14] encapsulated within $\{Mo_{132}\}$-type capsules. The presence of both internally bound and free valerates in aqueous solutions of **2** is further demonstrated by ^{1}H DOSY NMR spectroscopy (see Figure S4).

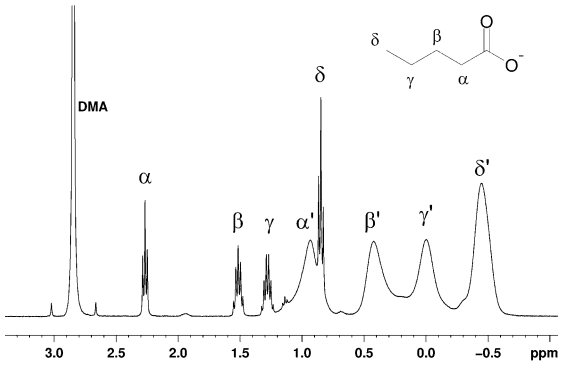

Figure 3. ^{1}H NMR spectrum of **2** (ca. 1 mM in D_2O) at room temperature.

Upon increasing the temperature to 363 K, the ROESY spectrum (Figure 4) ends up being a clear EXSY spectrum (Figure 5) that is dominated by a set of four groups of exchange signals of the type α⇄α′, β⇄β′, γ⇄γ′, and δ⇄δ′.

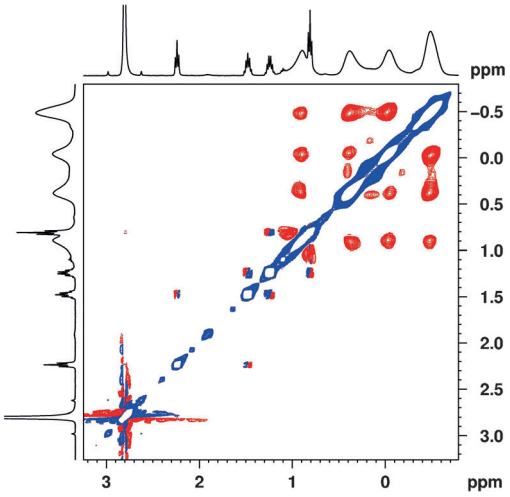

Figure 4. ^{1}H,^{1}H ROESY NMR spectrum of **2** (ca. 1 mM in D_2O) at room temperature. Negative ROE peaks are shown in red contours, relative to the positive diagonal peaks in blue (for details see Ref. [19]).

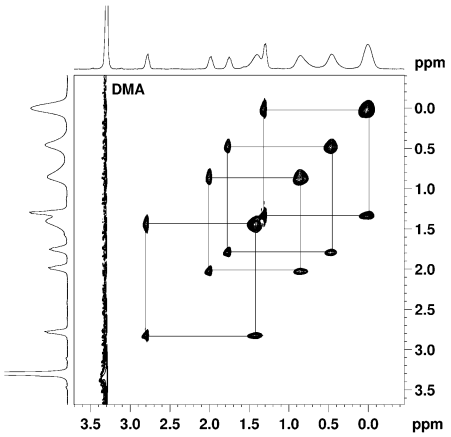

Figure 5. ^{1}H,^{1}H-EXSY spectrum of **2** (ca. 1 mM in D_2O) at 363 K (chemical shift variation due to temperature dependence).

After cooling back to room temperature, the ROESY spectrum is again obtained. This demonstrates high stability of the capsule, as well exchange between the internal and external valerates at high temperature. A deeper cut (see Figure S6) reveals some residual NOE signals, thus indicating that the exchange, although it is dominant at high temperature, is still slow enough to allow the observation of contacts between the confined hydrocarbon chains. This is different from the butyrate-type capsule[8a] and suggests that the exchange energy barrier is somewhat higher at this temperature than for butyrate (see Figures S6 to S8 for further details).

Additional observations reflect the remarkable stability of the valerate-type capsule in aqueous solution. First, the pH stability range of **2a** extends from approximately 0.5 to 7, which is broader than for the archetypal acetate-type capsule (ca. 2 to 6). Second, **2a** is almost inert toward replacement of the valerate ligands by sulfate ligands, which is in marked contrast to the behavior of carboxylate-type capsules containing shorter carbon chains, including butyrate (see the Supporting Information for details). These various features may be explained at least in part by the fact that the confined valerate aggregate blocks access to the cavity for external reagents (e.g., H_2O/OH^-, SO_4^{2-}).

In conclusion, a $\{Mo_{132}\}$-type capsule encapsulating a tightly packed $(valerate)_{24}$ aggregate was obtained by taking advantage of the unique reactivity of the carbonate-type capsule. It is noteworthy that as many valerate as butyrate ions could be accommodated within the cavity despite the increase in unfavorable steric repulsion, thus indicating a key role played by hydrophobic interactions (for further discussion, see the Supporting Information and Ref. [8b]). Looking at the whole series of carboxylate-containing $\{Mo_{132}\}$-type capsules now available, it is apparent that the more compact the encapsulate, the higher the stability of the whole system. A parallel can be drawn between encapsulated $(butyrate)_{24}$[8a] and $(valerate)_{24}$ aggregates and globular proteins, where the hydrophobic effect contributes to the stability by increasing packing density.[20] Although the $(valerate)_{24}$ and $(butyrate)_{24}$ assemblies bear some similarities, the valerate-type capsule **2a** is characterized by a denser and strongly crystallographically disordered organic core, as well as markedly diminished reactivity toward exchange between the inside and outside of the cavity.

Acknowledgements

A.M. acknowledges the Deutsche Forschungsgemeinschaft for continuous support and the ERC (Brussels) for an Advanced Grant. I.A.W. thanks the Israel Science Foundation for support (190/13). The authors thank Dr. Upendar Kashaboina (Bielefeld) for his contribution, Dr. Sayed Drweesh (Bielefeld) for preliminary preparation of an impure compound and Philip Saul M.Sc. (Hamburg) for repeating some NMR experiments.

Keywords: confinement effects · dense packing · hydrophobic interactions · NMR spectroscopy · porous capsules

How to cite: *Angew. Chem. Int. Ed.* **2016**, *55*, 6634 – 6637
Angew. Chem. **2016**, *128*, 6746 – 6749

[1] a) C. Tanford, *The Hydrophobic Effect: Formation of Micelles and Biological Membranes*, 2nd ed., Wiley, New York, **1980**; b) P. W. Snyder, J. Mecinović, D. T. Moustakas, S. W. Thomas III, M. Harder, E. T. Mack, M. R. Lockett, A. Héroux, W. Sherman, G. M. Whitesides, *Proc. Natl. Acad. Sci. USA* **2011**, *108*, 17889 – 17894.

[2] a) A. Müller, P. Gouzerh, *Chem. Eur. J.* **2014**, *20*, 4862 – 4873 (Concept Article); b) A. Müller, P. Gouzerh, *Chem. Soc. Rev.* **2012**, *41*, 7431 – 7463; c) H. N. Miras in *Discovering the Future of Molecular Sciences* (Ed.: B. Pignataro), Wiley-VCH, Weinheim, **2014**, pp. 189 – 215.

[3] C. Schäffer, A. M. Todea, P. Gouzerh, A. Müller, *Chem. Commun.* **2012**, *48*, 350 – 352.

[4] A. Ziv, A. Grego, S. Kopilevich, L. Zeiri, P. Miro, C. Bo, A. Müller, I. A. Weinstock, *J. Am. Chem. Soc.* **2009**, *131*, 6380 – 6382.

[5] a) A. Merca, E. T. K. Haupt, T. Mitra, H. Bögge, D. Rehder, A. Müller, *Chem. Eur. J.* **2007**, *13*, 7650 – 7658; b) E. T. K. Haupt, C. Wontorra, D. Rehder, A. Merca, A. Müller, *Chem. Eur. J.* **2008**, *14*, 8808 – 8811.

[6] A. Müller, S. Garai, C. Schäffer, A. Merca, H. Bögge, A. J. M. Al-Karawi, T. K. Prasad, *Chem. Eur. J.* **2014**, *20*, 6659 – 6664; cover profile: A. Müller, S. Garai, C. Schäffer, A. Merca, H. Bögge, A. J. M. Al-Karawi, T. K. Prasad, *Chem. Eur. J.* **2014**, *20*, 6561.

[7] a) C. Schäffer, A. M. Todea, H. Bögge, O. A. Petina, D. Rehder, E. T. K. Haupt, A. Müller, *Chem. Eur. J.* **2011**, *17*, 9634 – 9639; b) S. Kopilevich, H. Gottlieb, K. Keinan-Adamsky, A. Müller, I. A. Weinstock, *Angew. Chem. Int. Ed.* **2016**, *55*, 4476—4481; *Angew. Chem.* **2016**, *128*, 4552—4557.

[8] a) C. Schäffer, H. Bögge, A. Merca, I. A. Weinstock, D. Rehder, E. T. K. Haupt, A. Müller, *Angew. Chem. Int. Ed.* **2009**, *48*, 8051 – 8056; *Angew. Chem.* **2009**, *121*, 8195 – 8200; b) A. Grego, A. Müller, I. A. Weinstock, *Angew. Chem. Int. Ed.* **2013**, *52*, 8358 – 8362; *Angew. Chem.* **2013**, *125*, 8516 – 8520.

[9] D. Voet, J. G. Voet, *Biochemistry*, 4th ed., Wiley, New York, **2011**; see also other textbooks of biochemistry.

[10] a) B. van den Berg, *Curr. Opin. Struct. Biol.* **2005**, *15*, 401 – 407; b) E. M. Hearn, D. R. Patel, B. W. Lepore, M. Indic, B. van den Berg, *Nature* **2009**, *458*, 367 – 370.

[11] a) A. K. Dutta-Roy, *Cell. Mol. Life Sci.* **2000**, *57*, 1360 – 1372; b) R. L. Smathers, D. R. Petersen, *Hum. Genomics* **2011**, *5*, 170 – 191; c) M. Furuhashi, G. S. Hotamisligil, *Nat. Rev. Drug Discovery* **2008**, *7*, 489 – 503.

[12] S. Mosca, D. Ajami, J. Rebek, Jr., *Proc. Natl. Acad. Sci. USA* **2015**, *112*, 11181 – 11186.

[13] a) M. N. Ingale, V. V. Mahajani, *Sep. Technol.* **1994**, *4*, 252 – 257; b) S. K. Choudhari, F. Cerrone, T. Woods, K. Joyce, V. O'Flaherty, K. O'Connor, R. Babu, *J. Ind. Eng. Chem.* **2015**, *23*, 163 – 170.

[14] S. Garai, E. T. K. Haupt, H. Bögge, A. Merca, A. Müller, *Angew. Chem. Int. Ed.* **2012**, *51*, 10528 – 10531; *Angew. Chem.* **2012**, *124*, 10680 – 10683.

[15] Crystal data for **2**: $M = 28120.26\ \mathrm{g\,mol^{-1}}$, $C_{203}H_{1103}Mo_{132}N_{39}O_{710}$, rhombohedral, space group $R\bar{3}$, $a = 32.723(1)$, $c = 74.208(3)$ Å, $V = 68816(5)$ Å^3, $Z = 3$, $\rho = 2.036\ \mathrm{g\,cm^{-3}}$, $\mu = 15.21\ \mathrm{mm^{-1}}$, $F(000) = 41454$, crystal size $= 0.312 \times 0.303 \times 0.144\ \mathrm{mm^3}$. A total of 294955 reflections ($1.786 < \Theta < 72.504°$) were collected, of which 29898 reflections were unique ($R(\mathrm{int}) = 0.0591$). $R = 0.0639$ for 25323 reflections with $I > 3\sigma(I)$. $R = 0.0777$ for all reflections; max/min residual electron density 1.76 and $-1.52\ \mathrm{e\,Å^{-3}}$. The single crystals of **2** were coated with oil and measured at 100 K on a Bruker X8-Prospector Ultra diffractometer (three circle goniometer with 4 K CCD detector, Cu-Kα radiation, IμS microfocus source with multilayer optics; ω- and φ- scans). Empirical absorption corrections using equivalent reflections were performed with the program SADABS-2012/1 [G. M. Sheldrick, SADABS, University of Göttingen, Göttingen (Germany), 2003/12]. The structures were solved with the program SHELXS-2014 and refined using SHELXL-2014 integrated in Olex-2 software systems. Structure graphics were done with DIAMOND 2.1 from K. Brandenburg, Crystal Impact GbR, 2001. CCDC 1443656 (**2**) contains the supplementary crystallographic data for this paper. These data can be obtained free of charge from The Cambridge Crystallographic Data Centre.

[16] a) A. L. Spek, *J. Appl. Crystallogr.* **2003**, *36*, 7 – 13; b) A. L. Spek, *Acta Crystallogr. Sect. D* **2009**, *65*, 148 – 155.

[17] T.-L. Lai, M. Awada, S. Floquet, C. Roch-Marchal, W. Watfa, J. Marrot, M. Haouas, F. Taulelle, E. Cadot, *Chem. Eur. J.* **2015**, *21*, 13311 – 13320.

[18] O. Petina, D. Rehder, E. T. K. Haupt, A. Grego, I. A. Weinstock, A. Merca, H. Bögge, J. Szakács, A. Müller, *Angew. Chem. Int. Ed.* **2011**, *50*, 410 – 414; *Angew. Chem.* **2011**, *123*, 430 – 434.

[19] N. E. Jacobsen, *NMR Spectroscopy Explained*, Wiley, Hoboken, **2007**.

[20] B. W. Matthews, *Annu. Rev. Biochem.* **1993**, *62*, 139 – 160.

Received: February 1, 2016
Published online: May 3, 2016

